UDC 541.6:541.65:548.737

STRUCTURAL AND SPECTRAL PROPERTIES OF 3-SUBSTITUTEDPHENYL-1,5-DIPHENYLFORMAZANS: A QUANTUM CHEMICAL STUDY

H. Tezcan[1], N. Tokay[2]

[1]*Department of Chemistry, Faculty of Gazi Education, Gazi University, Ankara, Turkey*
[2]*Department of Chemistry, Faculty of Science, Hacettepe University, Ankara, Turkey*
 E-mail: habibe@gazi.edu.tr

The structural and optical properties of 3-substitutedphenyl-1,5-diphenylformazans are studied by quantum chemical methods. The density functional theory (DFT) is employed to optimize the ground state geometries of formazans substituted with different electron donating and withdrawing groups in both gas and solvent phases. The absorption spectra of formazan derivatives are calculated using time dependent density functional theory (TD-DFT). The polarizable continuum model (PCM) calculations of 3-substitutedphenyl-1,5-diphenylformazans are performed for bulk solvent effects. The geometrical parameters, vibrational frequencies, and relative stabilities of isomers of 3-substitutedphenyl-1,5-diphenylformazans are studied. The results obtained by TD-DFT calculations reveal that the substitution of electron withdrawing and donating substituents affects the absorption spectra of 3-substitutedphenyl-1,5-diphenylformazans. The calculated maximum absorption wavelengths (λ_{max}) are highly consistent with the experimental values as found from UV-vis spectra.

INTRODUCTION

In general, formazans are the focus of much interest in organic and medicinal chemistry because of their biochemical usefulness. The oxidation derivatives which penetrate various plant and animal tissues react with enzymes to form formazans and these molecules produce colored stains. This effect was investigated with idea that formazans might be important in view of their use in the determination of activity of tumor cells [1, 2], and the evalution of cytotoxicity of several compounds [3].

The molecular and electronic structures of formazans have attracted considerable experimental interest [4—7]. As a predictive tool for the structural properties, molecular modelization techniques allow a solution for the interpretation of experimental data. For the calculation of the electronic structures of many-particle systems, DFT is one of the most successful and widely used method in computational quantum chemistry, which can be a powerful theoretical tool in the design of dyes. In recent years, the time-dependent density functional theory (TD-DFT) has opened an efficient access to theoretical spectral absorption data in the visible and ultraviolet regions of the electromagnetic spectrum [8—10]. A limited number of DFT and TD-DFT investigations have been carried out on formazans [11, 12].

In this study, the maximum absorption wavelengths (λ_{max}) of 3-substitutedphenyl-1,5-diphenylformazans (Fig. 1) were studied with the help of TD-DFT quantum chemical calculations, and bulk
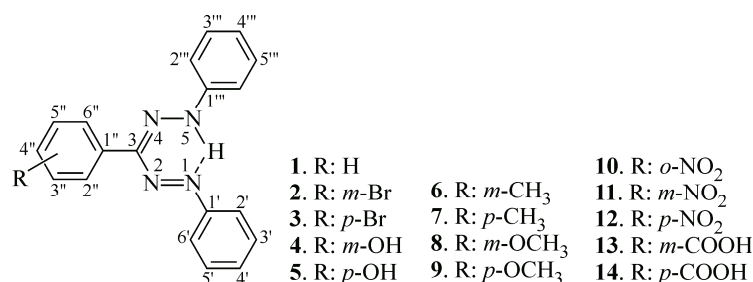
Fig. 1. Structures of 3-substitutedphenyl-1,5-diphenylformazans

solvent effects on singlet vertical excited states were investigated using the PCM method [13—16]. The calculated results were compared with the available experimental data.

COMPUTATIONAL METHOD

All calculations were carried out with the Gaussian 03 package program [17]. Quantum chemical calculations of **TPF** (**1**) have been performed by DFT using B3LYP [18—20], and PBE0 [21, 22] functionals with several basis sets to determine the best appropriate functional-basis set combination. A comparison of the experimental and calculated λ_{max} values of **TPF** revealed that the combination of the PBE0 functional with the 6-311G($2d$,$2p$) basis set was suitable. Taking into account this result, geometry optimizations of the studied compounds in the gas phase were carried out at the DFT level using PBE0/6-311G($2d$,$2p$) without any symmetry restrictions. Following each optimization, vibrational frequencies were calculated analytically to ensure them to be true local minima. Optimized geometries were used for the full geometry optimization in the solution. The bulk solvent effects have been modeled by PCM [13—16]. The equilibrium solvation has been selected to identify the equilibrium electronic structure and geometry.

The vertical excitation energy calculations were performed using the TD-DFT method [8—10] proved to be a powerful and effective computational tool for the study of the ground and excited state properties by comparing to the available experimental data. The calculations were carried out using the PBE0 functional with the 6-311G($2d$,$2p$) basis set on the previously optimized gas phase molecular geometries obtained at the same level of calculation. For the TD-DFT calculations, PCM was used to take into account the solvent effects.

RESULTS AND DISCUSSION

In order to determine the best functional and basis set combination for the λ_{max} calculation unsubstituted formazan 1,3,5-triphenylformazan **TPF** (**1**) was chosen. Buemi et al. [11] and King and Murrin [12] reported that there were many possible **TPF** conformations. In this study, the *trans-syn-s-cis* (TSSC) conformation was used for calculations because they found that the TSSC conformation had the global minimum.

Initially the optimized geometrical data for **TPF** were determined using some functionals with several basis sets. In order to ensure it to be a true local minimum, the optimized geometry was confirmed by a vibrational frequency calculation at the same level of theory. Then, the UV-vis data for **TPF** were obtained by the TD-DFT method with the same functionals and basis sets that were used for the geometry optimization. It was found that the combination of the PBE0 functional with the 6-311G($2d$,$2p$) basis set provided the best results [23].

Geometric structures and conformations. There are two possible conformation isomers for the *orto* [C2″(**a** type) and C6″ (**b** type)] and *meta* substitution [C3″ (**a** type) and C5″ (**b** type)] on the 3-phenyl ring (Fig. 1). The calculated Gibbs free energies of *orto* and *meta* substituted compounds are given in Table 1. The Gibbs free energies of **a** and **b** type isomers of compounds **2** (*m*-Br), **6** (*m*-CH$_3$), **8** (*m*-OCH$_3$), and **13** (*m*-COOH) are nearly the same. This is explained by the rotation of the 3-phenyl ring around the C3—C1″ single bond and by the repulsion of the 3- phenyl ring by 1- and 5-phenyl
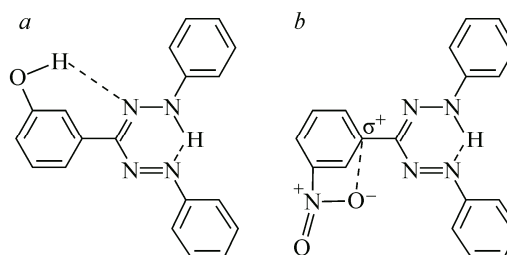
Calculated Gibbs free energies[a] (Hartree) *of o- and m-substituted compounds*

Subs type	Compound						
	2	4	6	8	10	11	13
a	–3524.703410	–1026.641265	–990.726950	–1065.874297	–1155.822895	–1155.833741	–1139.902796
b	–3524.703486	–1026.641867	–990.727209	–1065.874196	–1155.822223	–1155.833325	–1139.902833
b–a, eV	–0.0021	–0.0164	–0.0070	0.0027	0.0183	0.0113	–0.0010

[a] At PBE0/6-311G(2d,2p) level.

Fig. 2. Formation of weak attractive forces between OH and N4 (*a*) and NO$_2$ and C3 (*b*)

rings to the same directions. For compound **4** (*m*-OH), the stability of the **b** type isomer can be explained by the formation of a very weak H-bond between H of substituent OH and N4. It is not expected the formation of an H-bond between H of substituent OH and N2 because electrons are less intense in the C3—N2 single bond than in the C3=N4 double bond (Fig. 2, *a*). For NO$_2$-substituted compounds **10** (*o*-NO$_2$) and **11** (*m*-NO$_2$) **a** type isomers are more stable than **b** type. The great differences between the calculated Gibbs free energies of the isomers are caused by a strong electron withdrawing NO$_2$ group. The electrons on the 3-phenyl ring are strongly withdrawn by the NO$_2$ group. A weak attractive force can be formed between partially positively charged C3 and negatively charged oxygen atoms of NO$_2$ (Fig. 2, *b*).

The calculated Gibbs free energy of unsubstituted formazan **TPF** is –951.47134 Hartree (Table 1). It is observed that the substitution with different electron withdrawing and donating groups at *orto*, *meta*, or *para* positions of the 3-phenyl ring of **TPF**, decreases the Gibbs free energy because substituents increase the probability of the presence of the chelate structure and enforce the resonance of the main formazan skeleton. Therefore, substituted formazans are more stable than the unsubstituted one.

It has been noted that the Gibbs free energies of all studied compounds calculated at the B3LYP level have the same trend as observed at the PBE0 level.

The selected optimized geometrical parameters of 3-substitutedphenyl-1,5-diphenylformazans in the gas phase are given in Table 2. The stability of **TPF** can be explained by the conjugation within the pseudo six-membered ring, the chelate structure (Fig. 3). The formation of a hydrogen bond between the electron pair on the main skeleton (—N2=N̈1—∅) and the H atom bonded to N5 converts the structure to chelate and causes tautomerism [5]. The existence of the H-bond can be seen from the distance between the N1 and H atoms. It is found as 1.785 Å for **TPF**. In addition, the delocalization
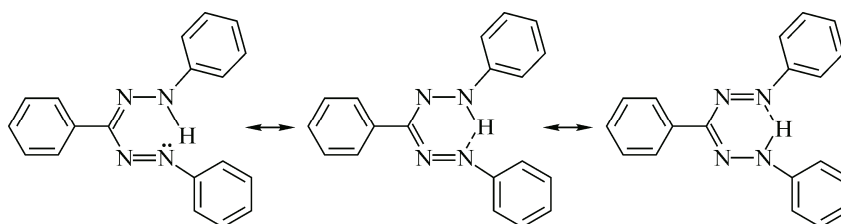

Fig. 3. Molecular chelation and tautomerism on **TPF** (**1**)

T a b l e   2

Selected optimized[a] *and experimental*[b] *geometrical parameters of* 3-*substitutedphenyl*-1,5-*diphenylformazans*

Com-pound	Bond length, Å					
	N1—N2	N2—C3	C3—N4	N4—N5	N5—H	N1···H
1	1.265	1.379	1.312	1.304	1.025	1.785
2	1.265	1.378	1.312	1.302	1.025	1.789
3	1.264	1.379	1.312	1.303	1.025	1.790
4	1.265	1.379	1.311	1.303	1.025	1.787
5	1.264	1.380	1.311	1.306	1.024	1.792
6	1.264	1.380	1.311	1.304	1.024	1.790
7	1.264	1.380	1.311	1.305	1.024	1.789
8	1.265	1.379	1.312	1.303	1.025	1.782
9	1.264	1.380	1.311	1.306	1.024	1.793
10	1.262	1.379	1.308	1.304	1.024	1.805
11	1.264	1.379	1.311	1.302	1.025	1.787
12	1.264	1.379	1.314	1.300	1.026	1.785
13	1.265	1.378	1.312	1.302	1.025	1.788
14	1.264	1.379	1.313	1.300	1.025	1.788
Exptl.	1.325	1.418	1.307	1.360	0.860	1.770

Com-pound	Dihedral angle, deg.				
	N1—N2—C3—N4	N5—N4—C3—N2	N2—N1—C1′—C6′	N2—C3—C1″—C2″	N4—N5—C1‴—C2‴
1	−1.0	−0.3	−9.3	−15.4	−3.5
2	−2.4	0.8	−9.5	−11.3	−2.1
3	1.4	0.0	10.4	14.5	3.4
4	−2.0	0.5	−10.0	−11.7	−2.5
5	−0.6	−0.9	−9.4	−15.3	−3.8
6	−0.3	1.0	8.6	15.0	3.6
7	1.0	0.4	9.9	14.8	3.7
8	−3.0	0.9	−13.0	−14.9	−2.9
9	1.3	0.4	9.9	14.2	3.7
10	−1.0	0.0	−14.4	32.2	1.6
11	1.4	−0.3	6.3	6.9	2.3
12	2.0	−0.6	10.0	10.3	3.0
13	−2.1	0.4	−9.8	−11.8	−2.5
14	−1.6	0.3	−10.6	−12.8	−3.2
Exptl.	−1.6	−3.2	3.1	165.1	−0.3

[a] For stable isomers at the PBE0/6-311G(2*d*,2*p*) level.
[b] [24].

in the ring can be explained by considering two C—N bond lengths. C3—N2 and C3—N4 bonds are found as 1.379 Å and 1.312 Å respectively. It is assumed that C3—N2 and C3—N4 bond lengths are nearly the same.

Some evidences in Table 2 show the existence of conjugation within the chelate structure in the studied compounds. Two of them have been seen for **TPF**. The first evidence is the presence of the H-bond in the structures of all compounds. The distances between N1 and H are about 1.79 Å for all structures. The other evidence is the C—N and N—N bond lengths to explain the delocalization

π-electrons in the main skeleton. C3—N2 and C3—N4 bond lengths are found as 1.379 Å and 1.312 Å respectively. It is assumed that C3—N2 and C3—N4 bond lengths are nearly the same. N1—N2 and N4—N5 bond lengths are found as 1.264 Å and 1.304 Å respectively. It can be said that N1—N2 and N4—N5 bond lengths are also similar. Another evidence is the observation of the planar main skeleton for all studied formazans. It can be seen from Table 2 that N1—N2—C3—N4 and N5—N4—C3—N2 dihedral angles are nearly zero. The maximum value is 3° for the first dihedral angle and 1° for the second.

In order to compare some selected optimized geometrical parameters with the experimental data X-ray data of 1-(4-bromophenyl)-3,5-diphenylformazan is needed. However, it has not been possible to have their appropriate single crystals. In the literature there is only the geometrical parameters of the 1-(4-bromophenyl)-3,5-diphenylformazan crystal [24]. It is accepted that the effect of the Br atom on the selected optimized geometrical parameters is negligible. It can be seen from Table 2 that the differences between optimized and experimental bond lengths are very small (~0.060 Å, ~0.040 Å, ~0.005 Å, ~0.060 Å, and ~0.010 Å for N1—N2, for N2—C3, for C3—N4, for N4—N5, andfor N1···H respectively). The highest difference is ~ –0.165 Å for N5—H. The differences between the optimized and experimental dihedral angles are very small. The difference is greater for N2—N1—C1'—C6'. This can be explained by the effect of the Br atom. It must be remembered that the optimized geometrical parameters are for the compounds in the gas phase and the experimental geometrical parameters are for the compound in the solid phase.

Lewis and Sandorfy [25] proposed that it is possible to explain a tautomeric structure of a compound by its IR spectra. The existence of chelation is supported by the position of the C=N stretching band in the spectrum:

a) the molecule has a chelate structure if the C=N stretching band is found at 1500—1510 cm^{-1};

b) there is no chelate structure if the C=N stretching band is observed at 1551—1565 cm^{-1}.

In our previous studies [7, 26, 27] the C=N stretching bands have been observed at 1490—1520 cm^{-1} for 1-substitutedphenyl- and 3-substitutedphenyl-diphenylformazans that form generally chelate structures.This agrees with the hypothesis that the repulsion of bulky groups attached to the 3-phenyl ring converts the main skeleton to a ring.

It is expected that all phenyl rings must be in the same plane also because of chelation. It can be seen from Table 2 that the phenyl groups bonded to N5 on the formazan skeleton are planar for all compounds. On the other hand, it is found that the phenyl groups bonded to N1 and C3 are out of the main skeleton of formazan. Because of the repulsion between substituted bulky groups and phenyl rings, N2—C3—C1″—C2″ dihedral angles are greater than the others. The substituted phenyl ring is tilted 32.2° due to great steric repulsion between NO$_2$ substituted at *orto* position and the phenyl group bonded to N1. N2—C3—C1″—C2″ dihedral angle for compound **11** with the NO$_2$ substituent at the *meta* position is smaller than that of **10** with NO$_2$ at the *orto* position because the repulsion decreases from the *orto* to *meta* position.

The effect of substitution on UV-vis spectra. The UV-vis spectra of formazans depend on both nature and positions of substituents. In order to see the effects of substituents on UV-vis spectra, the spectral studies of unsubstituted and substituted formazans are performed using the TD-DFT calculation at PBE0/6-311G(2d,2p) and B3LYP/6-311G(2d,2p) levels of theory in the gas and solvent phases. The solvent is chloroform with the dielectric constant $\varepsilon = 4.7113$. The experimental and calculated λ_{max} values, and the oscillator strengths are given in Table 3. A comparison of the λ_{max} values obtained at PBE0 and B3LYP levels shows that the absorption spectra of formazans are slightly shifted to a higher wavelength region for the B3LYP method. In addition, the experimental data are more compatible with the PBE0 results. The agreement between the experimental data and the calculated values is higher for the solvent phase than the gas phase at the PBE0 level for both electron donating and electron withdrawing substituents (Table 3).

Fig. 4 shows the comparison of calculated and experimental λ_{max} for 3-substitutedphenyl-1,5-diphenylformazans. The linear correlation between the experimental and calculated λ_{max} values of 3-substituted formazans yields a correlation coefficient r^2 of 0.96, and a mean absolute error (MAE) of

Experimental[a] *and calculated* λ_{max} (nm) *values and oscillator strengths f*
for all studied formazans

Com-pound	Exp. λ_{max}	Calculated							
		PBE0[b]				B3LYP[c]			
		gas		PCM[d]		gas		PCM	
		λ_{max}	f	λ_{max}	f	λ_{max}	f	λ_{max}	f
1	487	490	0.5651	**487**	0.5644	506	0.5377	501	0.5449
2a	488	483	0.5853	481	0.5839	499	0.5619	495	0.5721
2b		483	0.5788	**482**	0.5789	499	0.5550	499	0.5495
3	488	489	0.5578	**492**	0.5578	506	0.5313	503	0.5301
4a	480	494	0.4826	497	0.4792	512	0.4422	514	0.4446
4b		491	0.5357	**491**	0.5329	507	0.4986	508	0.4903
5	503	526	0.4114	**524**	0.4107	544	0.3419	544	0.2860
6a	489	491	0.5508	491	0.5492	508	0.5177	508	0.5194
6b		492	0.5465	**489**	0.5455	509	0.5176	510	0.5120
7	488	484	0.3915	**497**	0.5139	518	0.4852	515	0.4830
8a	488	497	0.4694	495	0.4610	517	0.3965	519	0.3994
8b		489	0.5535	**488**	0.5535	507	0.5129	508	0.4994
9	508	525	0.4197	**522**	0.4166	546	0.2326	546	0.1436
10a	410[e]	412	0.0838	**413**	0.0705	457	0.1041	453	0.0704
10b		468	0.6414	466	0.6525	452	0.1094	449	0.0899
11a	481[e]	485	0.5227	**481**	0.5133	503	0.4324	503	0.4137
11b		483	0.5131	480	0.5092	501	0.4140	503	0.4021
12	405[e]	403	0.5298	**406**	0.5397	432	0.4429	435	0.4676
13a	482[e]	485	0.5765	**482**	0.5756	500	0.5548	500	0.5520
13b		485	0.5665	479	0.5760	496	0.5584	497	0.5594
14	475[e]	477	0.6173	**476**	0.6132	492	0.5900	492	0.5870

[a] [26].

[b] TD-PCM-PBE0/6-311G($2d,2p$)//PCM-PBE0/6-311G($2d,2p$) level, solvent: $CHCl_3$.

[c] TD-PCM-B3LYP/6-311G($2d,2p$)//PCM-B3LYP/6-311G($2d,2p$) level, solvent: $CHCl_3$, but for the gas phase value for which the PCM model was not included.

[d] The bold values are considered for comparison.
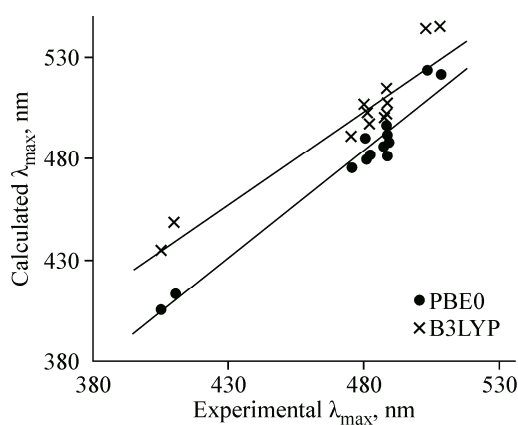
[e] Unpublished data.

Fig. 4. Comparison of experimental and calculated λ_{max} of the studied compounds

5.1 nm for PBE0. However, B3LYP yields r^2 of 0.89, and MAE of 23.7 nm. The minimum deviation between λ_{max} calculated at the TD-PCM-PBE0/6-311G(2d,2p)//PCM-PBE0/6-311G(2d,2p) level and experimental λ_{max} is 0 nm for **1** and **6**, and the maximum deviation is 21.1 nm for **5**.

Meta substitution of all substituents has no effect on the UV-vis spectra of 3-substitutedphenyl-1,5-diphenylformazans. There is no prominent resonance effect of substituents at the *meta* position of the 3-phenyl ring and the inductive effect is also weak.

As seen from Table 3, when the 3-phenyl ring is substituted by electron donating substituents (Br, CH$_3$, OCH$_3$) at *meta* and *para* positions, the shifts in λ_{max} values are higher (bathochromic effect) than those of **TPF**. The behavior of the Br substituent depends on two opposite effects: i) inductive electron withdrawing effect, and ii) resonance by the electron donating effect. It behaves as a very weak electron donor in this case. There is a small bathochromic shift, ranging 1—2 nm, in the case of CH$_3$ substitution at *meta* and *para* positions of 3-phenyl because CH$_3$ is a very weak electron donating group. A small bathochromic shift is also observed for OCH$_3$ substitution at *meta* position of 3-phenyl because of two opposite effects (inductive electron withdrawing and resonance by the electron donating effect). However, there is a significant bathochromic shift when the 3-phenyl ring is substituted by OCH$_3$ at the *para* position. This can be interpreted as the resonance effect of oxygen.

Substitution of 3-phenyl by NO$_2$ and COOH groups shift λ_{max} values to lower wavelengths (hypsochromic effect). This situation is compatible with the fact that NO$_2$ and COOH groups are electron withdrawing groups both inductively and in resonance. A comparison of λ_{max} values of COOH and NO$_2$ substituted formazans shows that the λ_{max} values of the first group are lower for all positions, because the COOH group has a lower electron withdrawing capacity than the NO$_2$ group.

It is well-known that the optical properties are directly related to the highest occupied molecular orbitals (HOMOs), lowest unoccupied molecular orbitals (LUMOs), and energy gaps. Table 4 lists the energies of the frontier orbitals of studied formazans calculated at the TD-PCM-PBE0/6-311G(2d,2p)//PCM-PBE0/6-311G(2d,2p) level. The results indicate that the main transition corresponds to $\pi \rightarrow \pi^*$ excitation for all studied formazans. For both unsubstituted and substituted formazans, the lowest energy transition is due to the electron excitation from HOMO to LUMO, except **10** and **11**. HOMO and LUMO of **TPF**, **5**, and **12** are depicted in Fig. 5. The frontier orbitals of substituted formazans are similar to those of **TPF**. When the frontier orbitals of **TPF** are analyzed, it can be seen that HOMO is distributed on the main molecular skeleton, while LUMO is localized on the Ph—N=N—C=N—N—Ph skeleton.

It is observed that HOMO-LUMO energy gaps for formazans which have electron donating substituents (Br, OH, CH$_3$, and OCH$_3$) at 3-phenyl decrease from *meta*-substituted compounds to their *para*-forms. For example, the gap values for *p*-OH and *p*-OCH$_3$ substituted compounds are 2.88 eV, 2.89 eV respectively and 3.04 eV, 3.05 eV respectively for their *meta*-substituted forms. This observation may be the result of resonance of the non-bonding electron pair as the dominant electron donating effect, and the disappearance of the inductive electron withdrawing effect. The greater conjugated

T a b l e   4

Frontier orbital energies (eV) *of studied formazans*[a]

Frontier orbitals	Compound													
	1	**2**	**3**	**4**	**5**	**6**	**7**	**8**	**9**	**10**	**11**	**12**	**13**	**14**
HOMO	−5.66	−5.77	−5.72	−5.63	−5.45	−5.76	−5.59	−5.66	−5.47	−5.88	−5.86	−5.93	−5.76	−5.85
LUMO	−2.62	−2.69	−2.68	−2.60	−2.57	−2.73	−2.59	−2.61	−2.58	−2.67	−2.77	−2.82	−2.68	−2.74
E[b]	−3.04	−3.08	−3.04	−3.04	−2.88	−3.03	−3.00	−3.05	−2.89	−3.22	−3.09	−3.11	−3.08	−3.11

[a] TD-PCM-PBE0/6-311G(2d,2p)//PCM-PBE0/6-311G(2d,2p) level, solvent: CHCl$_3$.
[b] E = LUMO – HOMO, the energy gap.

HOMO   LUMO
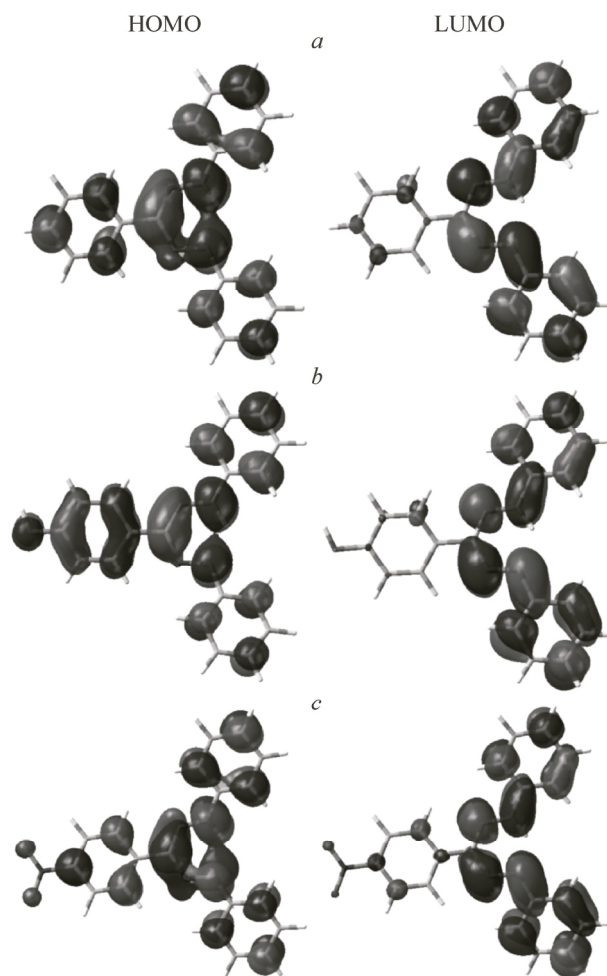
a

b

c

Fig. 5. Frontier orbitals of **1** (*a*), **5** (*b*), and **12** (*c*) (at the TD-PCM-PBE0/6-311G(2*d*,2*p*)//PCM-PBE0/6-311G(2*d*,2*p*) level)

part causes a less energy difference between HOMO and LUMO, and makes λ_{max} longer than *meta*-positions (bathocromic effect). However, for formazans having electron withdrawing substituents (NO_2 and COOH), the variation of MOs energies and HOMO-LUMO energy gaps are higher for *para*-substituted forms (3.11 eV for both groups) than for their *meta*-substituted forms (3.09 eV, 3.08 eV respectively). Therefore it is expected that *para*-substituted compounds absorb higher energies. The lower conjugated part causes a greater energy difference between HOMO and LUMO, and makes shorter λ_{max} than *meta*-positions (hypsochromic effect).

CONCLUSIONS

DFT and TD-DFT calculations were performed to investigate the geometrical and optical properties of unsubstituted and substituted 3-phenyl of 1,5-diphenylformazans by different electron withdrawing and donating groups in the gas and solvent phases. The calculated results indicated that the compounds possessed TSSC isomers because of the attached bulky groups on the 3-phenyl ring. They were able to remain essentially planar. The calculated C=N bond lengths and bond frequencies in the IR spectra indicated that the chelate structures were more stable than non-chelate ones.

Experimental data were more compatible with results for the solvent phase than for the gas phase at the PBE0 level for both electron donating and withdrawing substituents. 3-phenyl substituted formazans yielded r^2 of 0.96, and MAE of 5.1 nm for PBE0. However, B3LYP yielded r^2 of 0.89 and MAE of 23.7 nm.

The HOMO-LUMO energy gaps were less for the *para*-substituted electron donating groups (Br, OH, CH_3, OCH_3). The gaps especially for *para*-substituted OH and OCH_3 decreased more than the others. The greater conjugated part caused the lowering of the energy difference between HOMO and LUMO, and made λ_{max} longer according to *m*eta positions (bathochromic effect). However, for electron withdrawing substituents (NO_2 and COOH), HOMO-LUMO gaps increased from the *meta* position to the *para*position and made λ_{max} shorter according to the *meta* position (hypsochromic effect).

In summary, this study demonstrated that TD-PCM-PBE0 was a reliable method to investigate the geometrical and optical properties of formazans. There was good agreement between the calculated and experimental λ_{max} for the studied compounds.

REFERENCES

1. *Mattson A.M., Jensen CO., Dutcher R.A.* // Science. – 1947. – **5**. – P. 294 – 295.
2. *Stewart P.S., Griebe T., Srinivasan R.* // Appl. Environ. Microbiol. – 1994. – **60**. – P. 1690 – 1692.
3. *Yu F.P., Mcfeters G.A.* // Appl. Environ. Microbiol. – 1994. – **60**. – P. 2462 – 2466.
4. *Kohda K., Noda Y., Aoyama S., Umeda M., Sunino T., Kaiya T., Maruyama W., Naoi M.* // Chem. Res. Toxicol. – 1998. – **11**. – P. 1249 – 1253.
5. *Hunter L., Roberts C.B.* // J. Chem. Soc. – 1941. – **9**. – P. 820.

6. *Hegarty A.F., Scott F.L.* // J. Org. Chem. – 1967. – **32**. – P. 1957 – 1963.
7. *Tezcan H., Uzluk E.* // Dyes and Pigments. – 2007. – **75**. – P. 633 – 640.
8. *Runge E., Gross E.K.U.* // Phys Rev Lett. – 1984. – **52**. – P. 997 – 1000.
9. *Stratmann R.E., Scuseria G.E.* // J. Chem. Phys. – 1998. – **109**. – P. 8218 – 8224.
10. *Guillaumont D., Nakmura S.* // Dyes and Pigments. – 2000. – **46**. – P. 85 – 92.
11. *Buemi G., Zuccarello F., Venuvanalingam P., Ramalingam M., Ammal S.S.C.* // J. Chem. Soc. Faraday Trans. – 1998. – **94**. – P. 3313 – 3319.
12. *King R.A., Murrin B.J.* // Chem. Phys. – 2004. – **108**. – P. 4961 – 4965.
13. *Tomasi J., Persico M.* // Chem. Rev. – 1994. – **94**. – P. 2027 – 2094.
14. *Barone V., Cossi M., Mennucci B., Tomasi J.* // J. Chem. Phys. – 1997. – **107**. – P. 3210 – 3221.
15. *Cossi M., Barone V.* // J. Chem. Phys. – 2001. – **115**. – P. 4708 – 4717.
16. *Tomasi J., Mennucci B.R., Cammi R.* // Chem. Rev. – 2005. – **105**. – P. 2999 – 3093.
17. *Frisch M.J., Trucks G.W., Schlegel H.B., Scuseria G.E., Robb M.A., Cheeseman J.R., Montgomery Jr J.A., Vreven T., Kudin K.N., Burant J.C., Millam J.M., Iyengar S.S., Tomasi J., Barone V., Mennucci B., Cossi M., Scalmani G., Rega N., Petersson G.A., Nakatsuji H., Hada M., Ehara M., Toyota K., Fukuda R., Hasegawa J., Ishida M., Nakajima T., Honda Y., Kitao O., Nakai H., Klene M., Li X., Knox J.E., Hratchian H.P., Cross J.B., Bakken V., Adamo C., Jaramillo J., Gomperts R., Stratmann R.E., Yazyev O., Austin A.J., Cammi R., Pomelli C., Ochterski J.W., Ayala P.Y., Morokuma K., Voth G.A., Salvador P., Dannenberg J.J., Zakrzewski V.G., Dapprich S., Daniels A.D., Strain M.C., Farkas O., Malick D.K., Rabuck A.D., Raghavachari K., Foresman J.B., Ortiz J.V., Cui Q., Baboul A.G., Clifford S., Cioslowski J., Stefanov B.B., Liu G., Liashenko A., Piskorz P., Komaromi I., Martin R.L., Fox D.J., Keith T., Al Laham M.A., Peng C.Y., Nanayakkara A., Challacombe M., Gill P.M.W., Johnson B., Chen W., Wong M.W., Gonzalez C., Pople J.A.* Gaussian, Inc, Wallingford CT, 2004 Gaussian 03, Revision D.01.
18. *Becke A.D.* // Phys. Rev. – 1988. – **A38**. – P. 3098 – 3100.
19. *Becke A.D.* // J. Chem. Phys. – 1993. – **98**. – P. 5648 – 5652.
20. *Lee C.T., Yang W.T., Parr R.G.* // Phys. Rev. B. – 1988. – **37**. – P. 785 – 789.
21. *Perdew J.P.* // Phys. Rev. B. – 1986. – **33**. – P. 8822 – 8824.
22. *Perdew J.P., Burke K., Ernzerhof M.* // Phys. Rev. Lett. – 1996. – **77**. – P. 3865 – 3868.
23. *Tezcan H., Tokay N.* // Spect. Chim. Acta A. – 2010. – **75**. – P. 54 – 60.
24. *Tezcan H., Tokay N., Alpaslan G., Erdönmez A.* // Crystallogr. Rep. – 2013. – **58**. – P. 1107 – 1112.
25. *Lewis J.W., Sandorfy C.* // Can. J. Chem. – 1983. – **61**. – P. 809 – 816.
26. *Tezcan H., Can Ş., Tezcan R.* // Dyes and Pigments. – 2002. – **52**. – P. 121 – 127.
27. *Tezcan H., Özkan N.* // Dyes and Pigments. – 2003. – **56**. – P. 159 – 166.